

Diffusion of oxygen molecules in fluorine-doped amorphous SiO₂

Koichi Kajihara,^{1,2*} Taisuke Miura,³ Hayato Kamioka,⁴
Masahiro Hirano,^{1,6} Linards Skuja,^{1,5} and Hideo Hosono^{1,6}

¹ *Transparent Electro-Active Materials Project,
ERATO-SORST, Japan Science and Technology Agency,
in Frontier Research Center, S2-13,
Tokyo Institute of Technology, 4259 Nagatsuta,
Midori-ku, Yokohama 226-8503, Japan*

² *Department of Applied Chemistry,
Graduate School of Urban Environmental Sciences, Tokyo Metropolitan University,
1-1 Minami-Osawa, Hachioji 192-0397, Japan*

³ *Research & Development Division, OMRON Laserfront Inc.,
1120 Shimokuzawa, Sagami-hara 229-1198, Japan*

⁴ *Graduate School of Pure and Applied Sciences,
University of Tsukuba, 1-1-1 Tennodai, Tsukuba 305-8571, Japan*

⁵ *Institute of Solid State Physics, University of Latvia,
Kengaraga iela 8, LV1063 Riga, Latvia*

⁶ *Materials and Structures Laboratory & Frontier
Research Center, Tokyo Institute of Technology,
4259 Nagatsuta, Midori-ku, Yokohama 226-8503, Japan*

* Author to whom correspondence should be addressed; e-mail: kkaji@tmu.ac.jp

Abstract

Effects of fluorine doping on the diffusion of interstitial oxygen molecules (O_2) in amorphous SiO_2 (a - SiO_2) were compared to those obtained from a - SiO_2 containing SiOH groups. Incorporation of moderate concentration ($\sim 10^{19} \text{cm}^{-3}$) of SiF groups gives rise to minor changes in diffusion parameters between 800 and 1100°C: only a slight decrease in solubility and an increase in the activation energy for diffusion can be detected. Incorporation of SiOH groups has similar weak effects on the solubility and activation energy for diffusion. These minor changes are most likely due to the enhancement of the flexibility of local Si-O network as a result of the dissociation of the network by SiOH and SiF groups. However, in contrast to the SiF doping, SiOH doping leads to a notable decrease in the diffusion coefficient. The heat of solution changes by ~ 0.1 – 0.2 eV at $\sim 1000^\circ\text{C}$ and it is attributed to the glass transition of a - SiO_2 .

INTRODUCTION

Amorphous SiO₂ (*a*-SiO₂) is widely used as gate dielectric films for silicon microelectronic circuits, optical fibers for telecommunication, and optical components in excimer laser photolithography. Fluorine is one of the most important dopant for *a*-SiO₂ used as such devices, because moderate fluorine doping increases the radiation hardness of *a*-SiO₂ [1–4], suppresses the electrical breakdown of the gate dielectric films, and improves the optical transmittance near the absorption edge of *a*-SiO₂ located at $h\nu \simeq 8$ eV [5]. These improvements are mainly due to the breaking up of Si-O network by Si-F bonds. It decreases the viscosity of *a*-SiO₂ [3] and enhances the structural relaxation [6, 7], facilitating the removal of “strained” Si-O-Si bonds, which are considered to be a major source of point defects in *a*-SiO₂ [8–13]. Furthermore, Si-F bonds themselves are stronger than Si-O bonds that build the *a*-SiO₂ network and are hardly decomposed. Thus, radiation hardness of fluorine-doped *a*-SiO₂ is better than that of *a*-SiO₂ containing other network modifiers, such as SiOH and SiCl groups. Similarly to SiF groups they enhance the structural relaxation, however, they can be converted to point defects under radiation or electrical stress.

Oxygen molecules dissolved in interstices of Si-O network (interstitial O₂) are the main mobile oxygen species in *a*-SiO₂ [14–16]. They play a key role in thermal oxidation of silicon [17] and radiation induced defect processes in *a*-SiO₂ [18]. Interstitial O₂ in *a*-SiO₂ are sensitively detected by their characteristic infrared photoluminescence at ~ 1273 nm, attributed to the transition from the lower excited singlet state ($a^1\Delta_g$) to the ground state ($X^3\Sigma_g^-$) [19]. It is possible to detect as few as $\sim 10^{14}$ cm⁻³ interstitial O₂ when the upper excited singlet state ($b^1\Sigma_g^+$) is populated using a continuous-wave laser light at a wavelength of 765 nm [20]. The sensitivity is sufficient to detect interstitial O₂ incorporated during thermal annealing in air [21], offering an easy and straightforward way to quantitatively study the thermal diffusion of interstitial O₂ in *a*-SiO₂ [22]. Furthermore, this PL method is precise enough to evaluate the variations of the solubility and diffusion coefficient of interstitial O₂ with the incorporation of $\sim 10^{20}$ cm⁻³ SiOH groups [18, 23], which are the most common network modifiers in synthetic *a*-SiO₂.

The purpose of the present study is to examine the influence of the incorporation of SiF groups on the diffusion of interstitial O₂ in *a*-SiO₂ and to compare it with that of SiOH groups.

EXPERIMENTAL PROCEDURE

Fluorine-doped synthetic SiO₂ glass containing $\sim 1.4 \times 10^{19} \text{ cm}^{-3}$ of SiF groups and $\sim 1\text{--}2 \times 10^{18} \text{ cm}^{-3}$ of SiOH groups was cut into specimens in the form of $7 \times 10 \times 1 \text{ mm}^3$, and the two largest faces were polished to an optical finish. They were thermally annealed in air at 800, 900, 1000, or 1100°C to incorporate interstitial O₂. The PL band of interstitial O₂ in the O₂-loaded samples was excited at 765 nm using an AlGaAs laser diode ($\sim 1.5 \text{ W}$ at the sample position) and was measured using the detector part of a Fourier-transform Raman spectrometer (Model 960 Nicolet). The laser light was directed normal to the polished surface and the backscattered PL signal was recorded. The peak amplitude of the PL band is proportional to the thickness average of the concentration of interstitial O₂, C_a , and the proportionality factor was determined using a reference sample with a known O₂ concentration.

RESULTS

Figure 1 shows the variation of C_a with annealing time t at 800, 900, 1000, or 1100°C. C_a was proportional to $t^{1/2}$ at small t , and saturated at a constant value at large t . This observation indicates that the dissolution of O₂ from air is much faster than the following O₂ diffusion in *a*-SiO₂ [22] and is consistent with previous results [22, 23]. Thus, the observed variation of C_a with t was simulated well by an equation describing the simplest one-dimensional diffusion in a parallel sheet of a thickness L [24],

$$\frac{C_a(t)}{C_0} = 1 - \frac{8}{\pi^2} \sum_{n=1}^{\infty} \frac{\exp[-D(2n-1)^2\pi^2t/L^2]}{(2n-1)^2}, \quad (1)$$

using the diffusion coefficient D and the saturation concentration C_0 as adjustable parameters. The best-fit theoretical curves are shown as solid lines in Fig. 1. The solubility S was calculated from the relation $S = C_0/p_{\text{O}_2}$, where p_{O_2} is the partial pressure of O₂ in air at atmospheric pressure ($p_{\text{O}_2}=0.209 \text{ atm}$), provided that C_0 is proportional to p_{O_2} at this pressure range [15, 23].

The D and S values derived from the data shown in Fig. 1 are plotted in Fig. 2 and are referred to as “F-doped”. Both $\log D$ and $\log S$ were almost proportional to the reciprocal of the absolute temperature T , with slight deviations starting to appear above $\sim 1000^\circ\text{C}$ in

the S plot. Apart from the point at 1100°C in the S plot, these data were fitted to the simple Arrhenius-type relations

$$D = D_0 \exp(-\Delta E_a/kT), \quad (2)$$

$$S = S_0 \exp(-\Delta H/kT), \quad (3)$$

to evaluate the activation energy for diffusion ΔE_a , the heat of solution ΔH , and the pre-exponential factors D_0 and S_0 . k in Eqs. (2) and (3) denotes the Boltzmann constant. The calculated parameters are listed in Table I. The experimental uncertainties of ΔE_a and D_0 were larger for the F-doped sample than for the LowOH and HighOH samples reported previously [18, 23], because the temperature range used for the fitting of the F-doped sample data was narrower.

DISCUSSION

Figure 2 also shows D and S values of interstitial O_2 reported to date. The obtained ΔE_a , ΔH , D_0 , and S_0 values are listed in Table I, along with the measurement method, sample type, and abbreviated name. Agreements among data are good for D , ΔE_a , and ΔH . However, our S data are ~ 2.5 times smaller than those reported in Ref. [15].

The LowOH sample is fluorine-free and contains SiOH groups in concentration comparable with that in the F-doped sample. In these two samples the behavior of diffusion of interstitial O_2 is very similar, except for a subtly higher ΔE_a and smaller S in the F-doped sample. This observation indicates that incorporation of $\sim 10^{19} \text{ cm}^{-3}$ SiF groups does not significantly modify the diffusion of interstitial O_2 .

The diffusion of molecular species in solids has been studied well for amorphous organic polymers, and these results may provide insight into the diffusion of molecular species in $a\text{-SiO}_2$. In amorphous organic polymers, ΔH above the glass transition temperature (T_g) is generally larger (i.e., smaller by absolute value since ΔH is negative) than that below T_g [25]. It is explained by postulating that the main dissolution mechanism below T_g is exothermic trapping of molecules in relatively rigid interstitial voids. Above T_g , these voids are considered to be destroyed by the enhancement of the thermal motion of the network, indicating that heat to form voids is additionally needed to incorporate molecules. In $a\text{-SiO}_2$, a change in ΔH is observed at $\sim 1000^\circ\text{C}$ in all samples we measured [Fig. 2(b)]. All

these samples became deformed by viscous flow at 1200°C, indicating that T_g is lower than 1200°C. The measurements of the specific volume [26], the heat capacity [26, 27], and the light scattering intensity [28] show that T_g of α -SiO₂ is \sim 1000–1200°C, and that T_g decreases with an increase in the concentration of the network modifiers [28]. Although the reported T_g values are slightly higher than the observed change in ΔH at \sim 1000°C, we suggest that the ΔH change is due to the glass transition of α -SiO₂. Similar temperature difference can be observed for organic polymers with multiple relaxation processes [29]. Thus, the ΔH change may be related to structural rearrangements of local network domains (subrelaxation) below T_g , which is promoted by the presence of network modifiers, such as SiOH, SiF, and SiCl groups [30, 31].

The network modifiers dissociate the Si-O network and increase its flexibility, thus enhancing the local thermal motion around them [28]. This enhanced local thermal motion may collapse interstitial voids, with a mechanism similar to the destruction of the voids above T_g . The total concentration of the network modifiers in our samples increases in the order of LowOH, F-doped, and HighOH. This mechanism may explain the observed decrease in S in this order.

In amorphous organic polymers ΔE_a above T_g is generally larger than that below T_g . It is attributed to a larger jump distance of a molecule above T_g . A theory that describes the diffusion based on this mechanism predicts that the increase in ΔE_a is equal to ΔH above T_g minus ΔH below T_g [32]. However, the changes in ΔE_a actually observed for the diffusion of O₂ in poly(vinyl acetate) [33] and poly(ethylene terephthalate) [32] are \sim 1/2 of those expected by the theory. If similar mechanism were effective in α -SiO₂, the change in ΔE_a at T_g would be \sim 0.1 eV. Considering the number of the data points and the experimental uncertainty shown in Fig. 2(a), the changes in ΔE_a at T_g are no larger than \sim 0.1 eV in α -SiO₂ samples we measured. However, changes in ΔE_a less than \sim 0.1 eV cannot be excluded. Nonetheless, the observed increase in ΔE_a with an increase in the concentrations of the network modifiers may be related to the increase in the network flexibility caused by the incorporation of the network modifiers. Similar increase in ΔE_a with an increase in the concentration of SiOH groups is observed for the diffusion of He in α -SiO₂ [34].

Although SiF and SiOH groups play qualitatively similar roles in the dissolution and diffusion of interstitial O₂ as described above, their quantitative effect on D (i.e. dependence of D on the concentration of network modifiers) seems different. D of the F-doped sample

is almost equal to that of the LowOH samples between 800 and 1100°C, whereas D of the HighOH sample is markedly smaller. Although the difference may be partly due to the smaller ($\sim 1/7$) concentration of SiF groups in the F-doped sample than that of SiOH groups in the HighOH sample, these data imply that SiOH groups disturb the diffusion of interstitial O_2 more strongly than SiF groups. This difference can be attributed to the difference in chemical properties between SiOH and SiF groups, most likely the higher chemical activity of SiOH groups, such as their ability to form hydrogen bonds and participation in hydration-dehydration reactions. However, further studies are obviously needed to test this hypothesis.

CONCLUSIONS

Diffusion of interstitial oxygen molecules (O_2) in fluorine-doped synthetic amorphous SiO_2 (a - SiO_2) was examined. The results are compared with the data taken from a - SiO_2 containing SiOH groups and are analyzed in terms of the concentration of network modifiers (SiOH and SiF groups). The observations indicate that solubility decreases and the activation energy for diffusion increases with an increase in the concentration of network modifiers. A comparison of the results with those reported for amorphous organic polymers suggests that such changes in the solubility and the activation energy for diffusion are attributed to the promotion of the local thermal motion of the Si-O network, resulting from the incorporation of network modifiers that dissociates the Si-O network. The change of the heat of solution at $\sim 1000^\circ C$ is probably due to the glass transition of a - SiO_2 , where the temperature dependence of the local thermal motion is expected to change discontinuously. However, change in the activation energy for diffusion at the glass transition temperature was not above experimental uncertainty. The diffusion coefficient is decreased by SiOH doping whereas it is varied only slightly by SiF doping, possibly because SiOH groups are more chemically active than SiF groups.

-
- [1] K. Awazu, H. Kawazoe, and K. Muta, *J. Appl. Phys.* **69**, 4183 (1991).
- [2] K. Arai, H. Imai, J. Isoya, H. Hosono, Y. Abe, and H. Imagawa, *Phys. Rev. B* **45**, 10818 (1992).
- [3] M. Kyoto, Y. Ohoga, S. Ishikawa, and Y. Ishiguro, *J. Mater. Sci.* **28**, 2738 (1993).
- [4] K. Kajihara, M. Hirano, L. Skuja, and H. Hosono, *Mater. Sci. Eng. B* **161**, 96 (2009).
- [5] H. Hosono, M. Mizuguchi, H. Kawazoe, and T. Ogawa, *Appl. Phys. Lett.* **74**, 2755 (1999).
- [6] Y. Ikuta, S. Kikugawa, M. Hirano, and H. Hosono, *J. Vac. Sci. Technol. B* **18**, 2891 (2000).
- [7] K. Saito and A. J. Ikushima, *J. Appl. Phys.* **91**, 4886 (2002).
- [8] R. A. B. Devine and J. Arndt, *Phys. Rev. B* **39**, 5132 (1989).
- [9] R. A. B. Devine and J. Arndt, *Phys. Rev. B* **42**, 2617 (1990).
- [10] H. Imai, K. Arai, J. Isoya, H. Hosono, Y. Abe, and H. Imagawa, *Phys. Rev. B* **48**, 3116 (1993).
- [11] H. Hosono, Y. Ikuta, T. Kinoshita, K. Kajihara, and M. Hirano, *Phys. Rev. Lett.* **87**, 175501 (2001).
- [12] K. Awazu and H. Kawazoe, *J. Appl. Phys.* **94**, 6243 (2003).
- [13] K. Kajihara, M. Hirano, L. Skuja, and H. Hosono, *Phys. Rev. B* **78**, 094201 (2008).
- [14] R. H. Doremus, *Diffusion of Reactive Molecules in Solids and Melts* (John Wiley & Sons, New York, 2002).
- [15] F. J. Norton, *Nature* **191**, 701 (1961).
- [16] M. A. Lamkin, F. L. Riley, and R. J. Fordham, *J. Eur. Ceram. Soc.* **10**, 347 (1992).
- [17] B. E. Deal and A. S. Grove, *J. Appl. Phys.* **36**, 3770 (1965).
- [18] K. Kajihara, T. Miura, H. Kamioka, A. Aiba, M. Uramoto, Y. Morimoto, M. Hirano, L. Skuja, and H. Hosono, *J. Non-Cryst. Solids* **354**, 224 (2008).
- [19] L. Skuja and B. Güttler, *Phys. Rev. Lett.* **77**, 2093 (1996).
- [20] L. Skuja, B. Güttler, D. Schiel, and A. R. Silin, *Phys. Rev. B* **58**, 14296 (1998).
- [21] K. Kajihara, T. Miura, H. Kamioka, M. Hirano, L. Skuja, and H. Hosono, *J. Non-Cryst. Solids* **349**, 205 (2004).
- [22] K. Kajihara, T. Miura, H. Kamioka, M. Hirano, L. Skuja, and H. Hosono, *J. Ceram. Soc. Jpn.* **112**, 559 (2004).
- [23] K. Kajihara, H. Kamioka, M. Hirano, T. Miura, L. Skuja, and H. Hosono, *J. Appl. Phys.* **98**,

013529 (2005).

- [24] J. Crank, *The Mathematics of Diffusion*, 2 ed. (Oxford University Press, Oxford, 1975).
- [25] A. S. Michaels, W. R. Vieth, and J. A. Barrie, *J. Appl. Phys.* **34**, 1 (1963).
- [26] R. Brückner, *J. Non-Cryst. Solids* **5**, 123 (1970).
- [27] P. Richet and Y. Bottinga, *Geochim. Cosmochim. Acta* **48**, 453 (1984).
- [28] K. Saito and A. J. Ikushima, *Appl. Phys. Lett.* **70**, 3504 (1997).
- [29] Y. P. Yampolskii, Y. Kamiya, and A. Y. Alentiev, *J. Appl. Polym. Sci.* **76**, 1691 (2000).
- [30] A. J. Ikushima, T. Fujiwara, and K. Saito, *J. Appl. Phys.* **88**, 1201 (2000).
- [31] K. Saito and A. J. Ikushima, *Appl. Phys. Lett.* **73**, 1209 (1998).
- [32] A. S. Michaels, W. R. Vieth, and J. A. Barrie, *J. Appl. Phys.* **34**, 13 (1963).
- [33] P. Meares, *J. Am. Chem. Soc.* **76**, 3415 (1954).
- [34] J. E. Shelby, *J. Am. Ceram. Soc.* **55**, 61 (1972).
- [35] G. Hetherington and K. H. Jack, *Phys. Chem. Glasses* **5**, 147 (1964).
- [36] C. C. Tournour and J. E. Shelby, *Phys. Chem. Glasses* **46**, 559 (2005).
- [37] R. M. Barrer, *J. Chem. Soc.* **136**, 378 (1934).

FIG. 1: Variation of the thickness average of interstitial O₂ concentration C_a with annealing time t for 1mm-thick samples annealed in air at 800, 900, 1000, or 1100°C. The error bar indicates the experimental uncertainty. The inset shows the PL band of interstitial O₂ for samples annealed at 900°C.

FIG. 2: Arrhenius plots of the diffusion coefficient (a) and solubility (b) of interstitial O₂. Data taken from Refs. [15, 23, 35, 36] are also shown. The error bars indicate the experimental uncertainty for data obtained by our group (F-doped, LowOH, and HighOH). The dotted lines at $T \geq 1000^\circ\text{C}$ in panel (b) correspond to linear fits drawn to guide the eye.

TABLE I: Arrhenius parameters for the diffusion of interstitial O_2 obtained under different measurement conditions: D_0 , the diffusion preexponential factor; ΔE_a , the activation energy for diffusion; S_0 , the solubility preexponential factor; and ΔH , the heat of solution.

Reference	Abbreviated name	Measurement method	Sample type (concentration unit: cm^{-3})	Range ($^{\circ}\text{C}$)	D_0 (cm^2s^{-1})	ΔE_a (eV)	S_0 ($\text{cm}^{-3} \text{atm}^{-1}$)	ΔH (eV)
This work	F-doped O_2 PL		SiF $\sim 1.4 \times 10^{19}$, SiOH $\sim 1-2 \times 10^{18}$	800–1100	$7.2 \times 10^{-5 \pm 0.3}$	0.98 ± 0.07	$3.9 \times 10^{15 \pm 0.2(a)}$	$-0.18 \pm 0.03^{(a)}$
Ref. [23]	LowOH O_2 PL		SiOH $\sim 2 \times 10^{18}$	800–1200	$4.5 \times 10^{-5 \pm 0.2}$	0.93 ± 0.05	$4.2 \times 10^{15 \pm 0.2(a,b)}$	$-0.18 \pm 0.03^{(a)}$
Ref. [23]	HighOH O_2 PL		SiOH $\sim 1 \times 10^{20}$, SiCl $\sim 5 \times 10^{18}$	800–1200	$6.7 \times 10^{-5 \pm 0.2}$	1.01 ± 0.05	$4.8 \times 10^{15 \pm 0.2(a,b)}$	$-0.15 \pm 0.03^{(a)}$
Ref. [37]	Permeation			680–944		$\sim 1.2^{(c)}$		
Ref. [15]	Permeation			950, 1078	2.7×10^{-4}	1.17	7.6×10^{15}	-0.22
Ref. [35]	Si-Si oxidation		IR Viterosil (contain Si-Si, low SiOH)	1050				
Ref. [36]	O_2 to SiOH conversion	Suprasil W	(contain O_2 , SiOH $< 4 \times 10^{17}$)	900–1200	1.2×10^{-5}	0.79		

^(a) Calculated from data at 1000 $^{\circ}\text{C}$ or less.

^(b) Updated from Ref. [23] with the thermal desorption data reported in Ref. [18].

^(c) Calculated by least squares fit of the data listed in Table 2 of Ref. [37]. The fit was performed above 700 $^{\circ}\text{C}$.

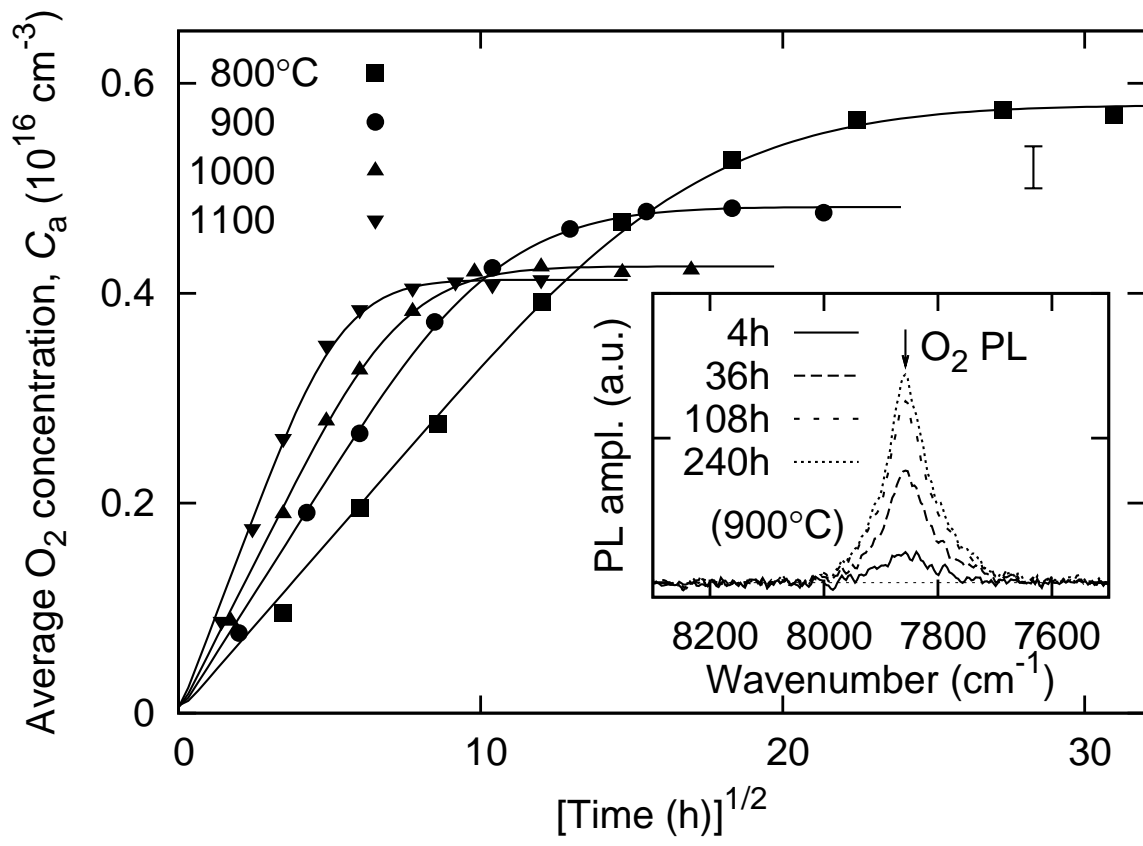


Fig.1 K. Kajihara et al.

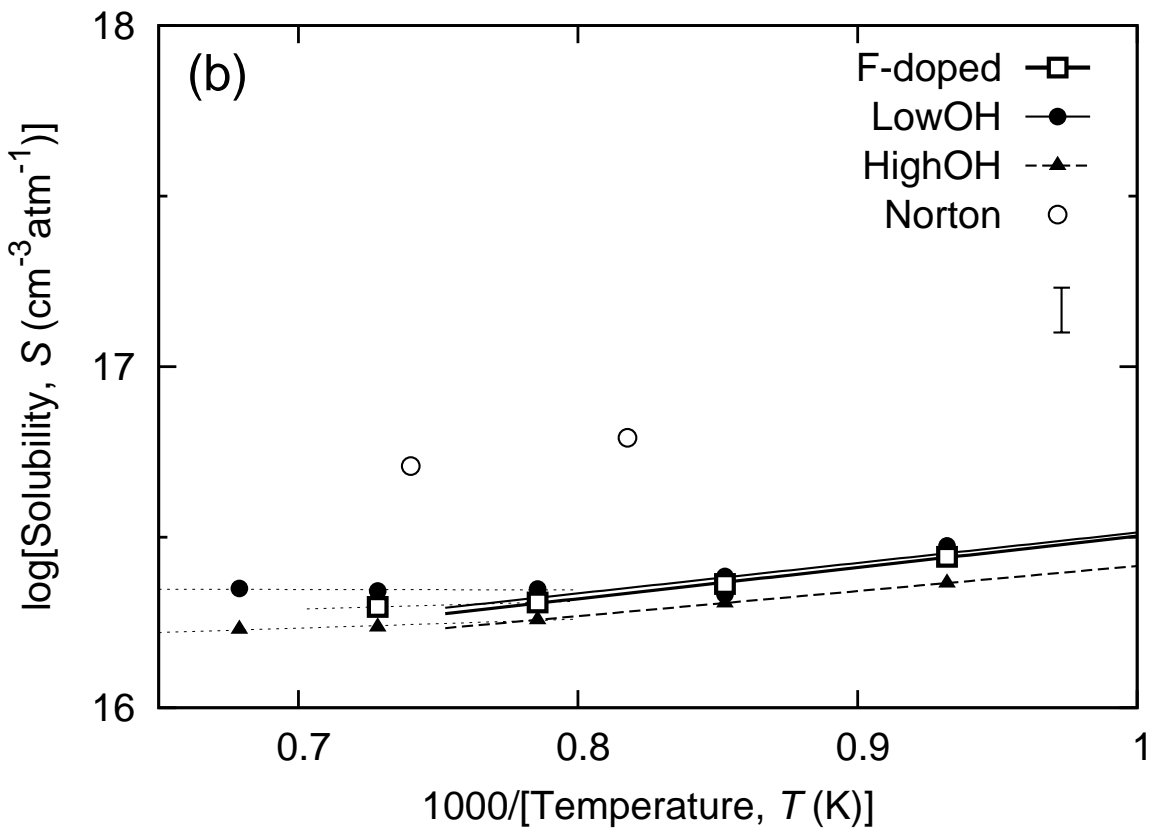
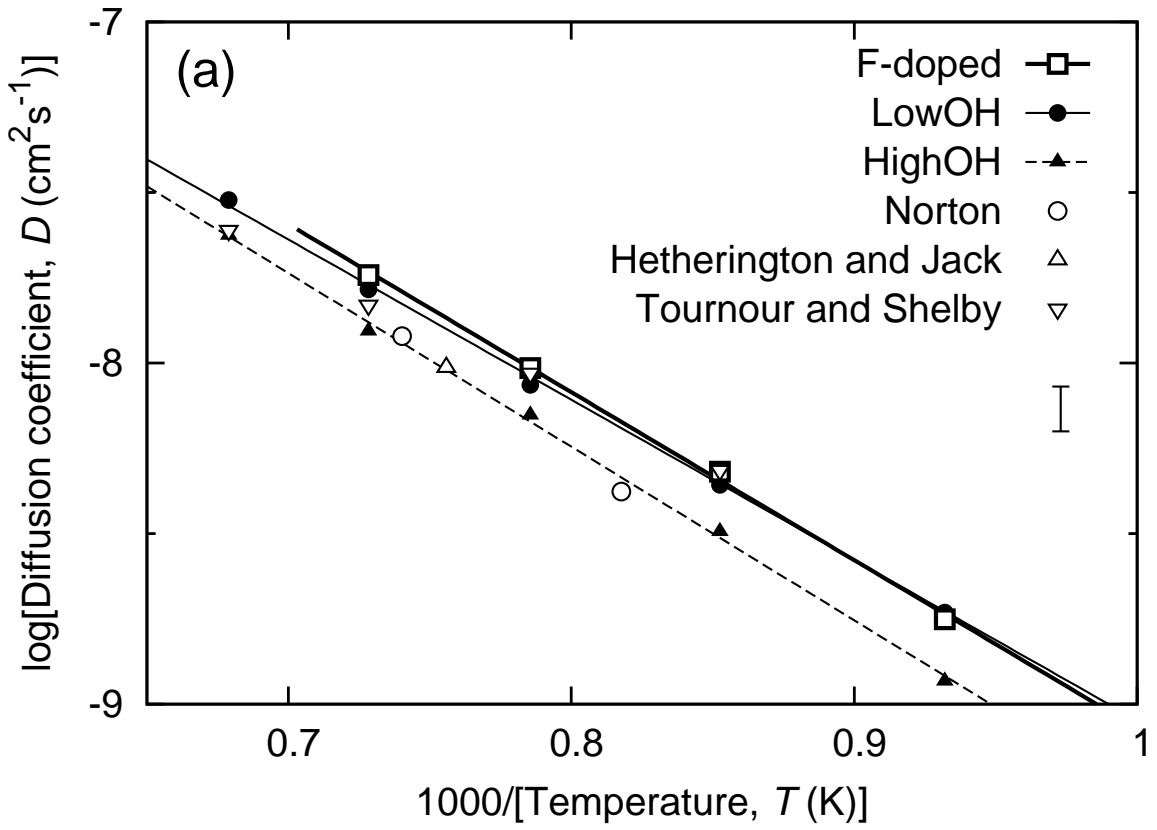


Fig.2 K. Kajihara et al.